Angle-resolved photoemission study of $Ga_{1-x}Mn_xAs$

J. Okabayashi,[1] A. Kimura,[2] O. Rader,[3] T. Mizokawa,[1] A. Fujimori,[1] T. Hayashi,[4] and M. Tanaka[4]

[1]*Department of Physics and Department of Complexity Science and Engineering, University of Tokyo, Bunkyo-ku, Tokyo 113-0033, Japan*

[2]*Department of Solid State Physics, Hiroshima University, Higashi, Hiroshima 739-8526, Japan*

[3]*BESSY, Albert-Einstein-Strasse 15, D-12489 Berlin, Germany*

[4]*Department of Electronic Engineering, University of Tokyo, Bunkyo-ku, Tokyo 113-0033, Japan*

Valence-band dispersions in $Ga_{1-x}Mn_xAs$ along the Γ-Δ-X line ($k\|[001]$) are obtained by angle-resolved photoemission spectroscopy. Compared with the spectra of GaAs, a small energy shift caused by Mn doping is observed for one of the valence bands. In addition, states are observed near the Fermi level in $Ga_{1-x}Mn_xAs$. These states show no clear dispersions and behave like an impurity band induced by Mn doping.

Diluted magnetic semiconductors (DMS) have attracted much attention because of the combination of magnetic and semiconducting properties and hence high potential for new device applications.[1] Recently DMS based on III-V compounds have been extensively studied because of the success in doping high concentrations of transition-metal ions by molecular beam epitaxy (MBE). Especially Mn doping in GaAs and InAs leading to ferromagnetism and interesting magnetotransport properties has attracted considerable interest in recent years.[2,3] This behavior is generally called "carrier-induced ferromagnetism" because hole carriers are introduced into the system by the Mn doping, however, its microscopic mechanism has been controversial until now.

In the Mn-doped DMS, the basically localized Mn $3d$ electrons interact with the itinerant band electrons of the host semiconductor. Strong Coulomb repulsion among the localized Mn $3d$ electrons and hybridization between the Mn $3d$ and the host semiconductor electrons have to be considered explicitly to clarify the origin of the carrier-induced ferromagnetism.[4] In the previous studies,[4] we have measured angle-integrated valence-band photoemission spectra and core-level photoemission spectra of $Ga_{1-x}Mn_xAs$ with subsequent analyses using configuration-interaction cluster-model calculations. The results have indicated that states just below the Fermi level (E_F) are due to a Mn $3d$ hole screened by charge transfer from the As $4p$ orbitals in the photoemission final state. That is, the states just below E_F have predominantly As $4p$-hole character with strongly hybridized Mn $3d$ component. According to first-principles calculation on a hypothetical zinc-blende type $Ga_{0.5}Mn_{0.5}As$ (supercell) by Shirai *et al.*,[6] the dominant component near E_F is As $4p$ orbitals and strong hybridization between the Mn $3d$ and As $4p$ states causes the ferromagnetism, consistent with the conclusion from the photoemission studies. On the other hand, band-structure calculation on $In_{1-x}Mn_xAs$ with the coherent potential approximation[5] (CPA) has indicated that the states near E_F have mainly Mn $3d$ character and that competition between the superexchange and double-exchange interactions between the Mn $3d$ electrons explains the magnetic properties. In order to clarify the electronic structure near E_F, we have performed angle-resolved photoemission spectroscopy (ARPES) studies of $Ga_{1-x}Mn_xAs$ in the present work.

ARPES is a powerful technique to study band dispersions in solids[7] and may give a key to explain the anomalous magnetotransport properties of the DMS.[8] In this work, ARPES studies have been performed for MBE-grown $Ga_{1-x}Mn_xAs$ (001) thin films. Mn-induced changes in the electronic band structure are observed near E_F as well as in deeper valence bands. ARPES measurements of GaAs were performed by many groups in the past for (110) [Refs. 9,10] and (001) [Ref. 11] surfaces. The (110) surface is the most studied surface of GaAs because it is a cleavage plane although the (001) surface has been most frequently used in technological applications. GaAs and $Ga_{1-x}Mn_xAs$ have the fcc zinc-blende structure. Important symmetry lines in the fcc Brillouin zone are the [001] (Γ-Δ-X), the [110] (Γ-Σ-K-X), and the [111] (Γ-Λ-L) directions.

Samples used in this experiment were a GaAs (001) substrate and $Ga_{1-x}Mn_xAs$ (001) epitaxial films with $x=0.035$ and 0.069 grown on it. The lattice constants of GaAs, $Ga_{0.965}Mn_{0.035}As$ and $Ga_{0.931}Mn_{0.069}As$ are $a=5.65$ Å, $a=5.67$ Å, and $a=5.69$ Å, respectively.[12,13] Experiment was done at beamline BL 18-A of Photon Factory, High Energy Accelerator Research Organization, using an ADES-500 spectrometer. The angular resolution was $\pm1°$ and the total energy resolution was 100 meV because the measurements were done at room temperature. Photoemission measurements were performed in an ultrahigh vacuum of 10^{-11} Torr. Light was incident on the sample with an incident angle of 45° with respect to the surface normal (and therefore the p and s polarization were mixed). Electrons emitted in the surface normal direction, which come from the Γ-Δ-X line, were collected. To remove oxidized surface layers and other contaminations, we made repeated Ar sputtering and annealing. GaAs can be heated up to 660 °C,[14,15] which is the evaporation temperature of Ga and As, and surface ordering changes according to the annealing and growth conditions.[16,17] In our experiment, however, the GaAs sample was heated only up to 240 °C in order to compare with $Ga_{1-x}Mn_xAs$, which was heated to 240 °C in order to avoid the decomposition into GaAs and MnAs particles. After the annealing, we confirmed ordered surfaces by observing 1×1 low-energy electron diffraction (LEED) patterns.
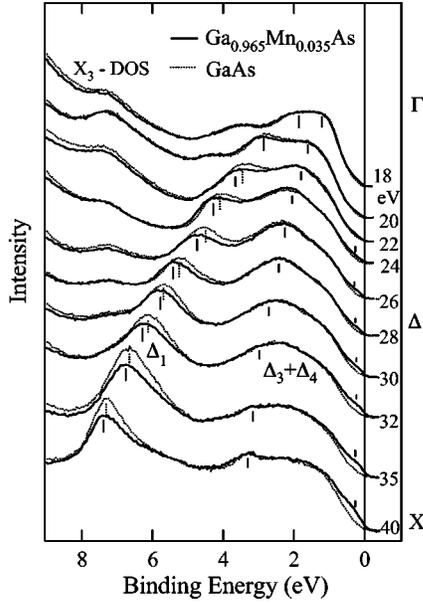
FIG. 1. Angle-resolved photoemission spectra of $Ga_{0.965}Mn_{0.035}As$ (solid curves) and GaAs (dash curves) along the Γ-Δ-X ([001]) direction. Vertical bars show peak or shoulder positions.

Figure 1 shows the normal emission spectra of GaAs (001) and $Ga_{1-x}Mn_xAs$ (001) with $x = 0.035$ along the Γ-Δ-X ([001]) direction. The Γ point can be measured with $h\nu \sim 10$ eV, according to the direct-transition model for ARPES with an appropriate inner potential.[9] Unfortunately electrons emitted with such low kinetic energies could not be detected well using our setup. The X point could be measured with ~ 35 eV. The peaks in Fig. 1 correspond to the Δ_1 band (split-off band) and the $\Delta_3 + \Delta_4$ bands (heavy- and light-hole bands, respectively) along the Γ-Δ-X line. The spectra have been normalized to the height of the $\Delta_3 + \Delta_4$ feature. The line shapes for GaAs are almost the same as those measured in Ref. 11. In our measurement, however, because the annealing temperature was as low as that used for $Ga_{1-x}Mn_xAs$, we could not observe very clearly the surface state at 1 eV binding energy. Figure 1 shows a weak shoulder around 1 eV, which is the contribution from the surface state and/or momentum (k) nonconserving transitions (secondary cone emission) from the Γ point and broadening of spectra would come from disorder at the surface. A trace of emission from the X_3 point is also observed at ~ 7 eV in all the spectra due to k-nonconserving transitions. It should be remembered that the emission from the X_3 point gives a strong peak in angle-integrated photoemission spectra.[4] Compared with GaAs, only the Δ_1 peak in $Ga_{1-x}Mn_xAs$ is shifted downward by 0.1–0.2 eV. The shift is negligibly small at the Γ and X points but is significant in between. Between E_F and 0.5 eV below it, the emission intensity increases in going from GaAs to $Ga_{1-x}Mn_xAs$, which we attribute to states induced by Mn doping near the valence-band maximum. Here, the zero of energy, that is E_F, has been determined by the Fermi edge of a Ta foil in electrical contact with the samples. These states may be derived from the acceptor level of the neutral Mn impurity (A^0) in
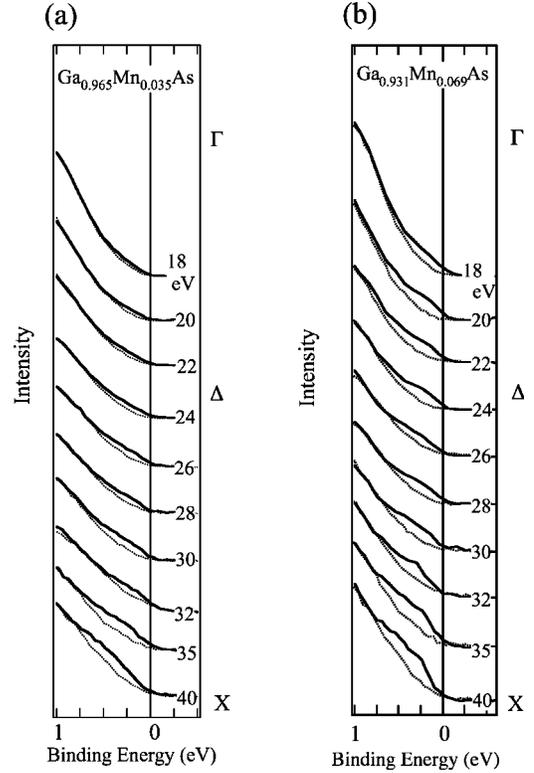
GaAs, which is located above the valence-band maximum by about 100 meV [Ref. 18] and may be viewed as Mn impurity states derived from the acceptor level.

Photoemission spectra near E_F are shown in Fig. 2 for $Ga_{0.965}Mn_{0.035}As$ and $Ga_{0.931}Mn_{0.069}As$ overlayed with the GaAs spectra. One can clearly see Mn-doping effects as the Mn-induced states between E_F and 0.5 eV. Using the spectra shown in Fig. 1, one can perform a band mapping in the energy momentum (E_i-k_i) plane of the initial states. We have used the work function of $\phi = 5$ eV and the "inner potential" of $E_0 = 7.7$ eV, the values reported for GaAs in Ref. 11. In order to emphasize the spectral features, we have taken the second derivatives of the spectra and plotted them on the gray scale. Figures 3(a) and 3(b) show the band dispersions for $Ga_{0.965}Mn_{0.035}As$ and GaAs thus obtained and plotted on the gray scale. One can see that the Δ_1 band in $Ga_{1-x}Mn_xAs$ is somewhat more strongly curved than that in GaAs, reflecting the Mn-induced shift of this band as described above. This shift is more clearly seen in Fig. 3(c), where the peak positions and other spectral features are plotted on the same panel. Unfortunately, it was difficult to recognize the Mn-induced states on the gray scale plot. Therefore, in order to show these states more clearly, the difference spectra between $Ga_{0.965}Mn_{0.035}As$ and GaAs are plotted in Fig. 3(d). The plot shows that the Mn-induced states form "impurity band states" just below E_F in $Ga_{1-x}Mn_xAs$. The impurity band does not show appreciable dispersion but a small dispersion of a few 100 meV cannot be excluded from the experimental data.
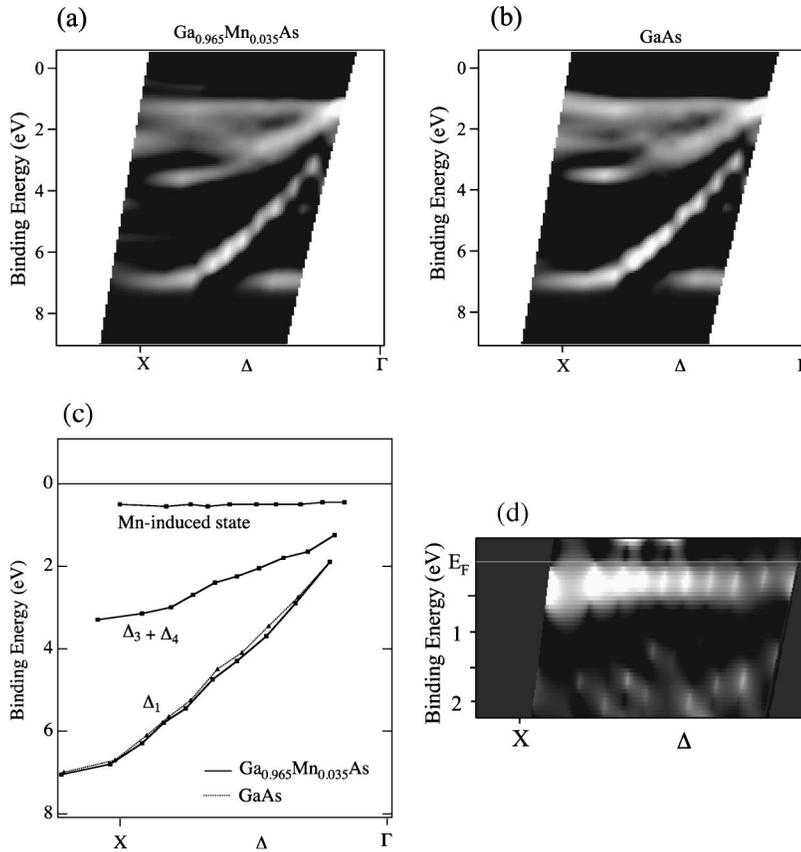

FIG. 2. Angle-resolved photoemission spectra near E_F of GaAs (dash curves) and $Ga_{1-x}Mn_xAs$ with $x = 0.035$ (a) and $x = 0.069$ (b) (solid curves).

FIG. 3. Experimental band structures of Ga$_{0.965}$Mn$_{0.035}$As (a) and GaAs (b) along the Γ-Δ-X direction from the ARPES measurements. Second derivatives of the spectra are plotted in the E_i-k_i plane on the gray scale. (c) Positions of spectral features plotted on the same scale as (a) and (b). (d) Difference spectra between Ga$_{0.965}$Mn$_{0.035}$As and GaAs, which show almost nondispersive Mn-induced features just below E_F.

The Mn-induced states near E_F should be responsible for the metallic conduction in Ga$_{1-x}$Mn$_x$As and would be the origin of the carrier-induced ferromagnetism and the anomalous magnetotransport properties. If the states induced by the Mn doping are derived from the acceptor level, which is originally located above E_F, large part of the impurity states would be located above E_F and ARPES sees only the bottom part of these states. From the previous cluster-model analysis,[4] dominant components near E_F in the photoemission spectra come from a Mn $3d$ hole screened by charge transfer of a host valence electron ($d^5\underline{L}$ photoemission final state, where $\underline{L}$ denotes a hole in the As $4p$ valence band), because the original Mn $3d$ level is located far (~ 4.5 eV) below E_F. According to the Anderson-impurity model calculation, the neutral Mn in GaAs may induce a split-off state above the valence-band maximum through hybridization with As $4p$ states[19,20] and act as an acceptor. Therefore the wave functions of the states would have mainly As $4p$ character with hybridized Mn $3d$ character but has the same symmetry as the Mn $3d$ orbitals with respect to the Mn site. Due to the hybridized Mn $3d$ character, their photoemission cross section increases with increasing photon energy following that of the Mn $3d$ atomic orbital, consistent with the photon energy dependence shown in Fig. 2. The Mn $3d$ component, although not dominant, would lead to the spin polarization of the impurity states. That is, the spin of the holes in the "impurity band" is coupled to the spin of the Mn $3d^5$ configuration, and thus contributes to the magnetotransport phenomena in Ga$_{1-x}$Mn$_x$As. According to the cluster-model analysis, the coupling between the spin of the hole in the

impurity band and the Mn spin is antiferromagnetic.[4] The mechanism of the formation of the impurity states is analogous to that of the Zhang-Rice singlet in the high-T_c cuprates,[21] where a hole in the O $2p$ band is antiferromagnetically coupled to the Cu $3d^9$ spin. The same scenario has been discussed for the DMS.[22,23] The Δ_1 band in Ga$_{1-x}$Mn$_x$As is shifted to higher binding energies possibly as a result of the hybridization with the Mn $3d$ states. It should be noticed that the "impurity band" has a finite but low spectral weight at E_F and is spread over $0.5-1$ eV from E_F. This behavior is similar to the doping-induced states in La$_{1-x}$Sr$_x$MnO$_3$ and implies a highly incoherent nature of the metallic states in Ga$_{1-x}$Mn$_x$As. Disorder effects due to Mn atom substitution may also contribute to the incoherent nature of the metallic state in Ga$_{1-x}$Mn$_x$As.

In order to further discuss the nature of the doping-induced states near E_F, we compare our result with the band structure calculated using CPA reported in Ref. 5. The calculation indeed predicts a dispersionless band at E_F induced by Mn doping as well as the downward shift of the Δ_1 band by ~ 0.5 eV. However, the calculation indicates that the carrier-induced ferromagnetism comes from the double-exchange mechanism competing with superexchange interaction and that the conduction takes place via the Mn $3d$ states. This does not agree with the observation in our photoemission studies that resonant photoemission spectra show little Mn $3d$ character near E_F.[4] On the other hand, a new band-structure calculation using the local-density approximation with Coulomb interaction (so-called LDA$+U$ method) shows low Mn $3d$ weight at E_F,[24] in agreement with the

conclusion from the photoemission studies. In this calculation, large contribution to the density of states near E_F comes from As $4p$ character, and itinerant As $4p$ states induce the ferromagnetic interaction between the Mn $3d$ ions through the p-d exchange interaction, consistent with the photoemission results.

In conclusion, we have investigated the band dispersions for $Ga_{1-x}Mn_xAs$ along the Γ-Δ-X direction in the Brillouin zone. Only the Δ_1 band shows a shift with Mn doping as a result of hybridization with the Mn $3d$ states. We have also observed ''impurity band states'' near E_F, which are also induced by the hybridization of the host valence-band states with the Mn $3d$ states. To clarify the nature of the ''impurity band states'' and their role in the carrier-induced ferromagnetism and the magnetotransport properties, detailed composition- and temperature-dependent photoemission studies with better energy resolution would be highly desired.

[1] H. Ohno, Science **281**, 951 (1998).

[2] H. Munekata, H. Ohno, S. von Molnar, A. Segmuller, L. L. Chang, and L. Esaki, Phys. Rev. Lett. **63**, 1849 (1989).

[3] H. Ohno, H. Munekata, T. Penny, S. von Molnar, A. Segmuller, and L. L. Chang, Phys. Rev. Lett. **68**, 2664 (1992).

[4] J. Okabayashi, A. Kimura, T. Mizokawa, A. Fujimori, T. Hayashi, and M. Tanaka, Phys. Rev. B **59**, R2486 (1999); J. Okabayashi, A. Kimura, O. Rader, T. Mizokawa, A. Fujimori, T. Hayashi, and M. Tanaka, *ibid.* **58**, R4211 (1999).

[5] H. Akai, Phys. Rev. Lett. **81**, 3002 (1998); (unpublished).

[6] M. Shirai, T. Ogawa, I. Kitagawa, and N. Suzuki, J. Magn. Magn. Mater. **177-181**, 1383 (1998).

[7] S. Hüfner, *Photoelectron Spectroscopy* (Springer-Verlag, Berlin, 1995).

[8] A. Oiwa, S. Katsumoto, A. Endo, M. Hirasawa, Y. Iye, H. Ohno, F. Matsukura, A. Shen, and Y. Sugawara, Solid State Commun. **103**, 209 (1997).

[9] T. C. Chiang, J. A. Knapp, M. Aono, and D. E. Eastman, Phys. Rev. B **21**, 3513 (1980).

[10] T. C. Chiang, J. A. Knapp, D. E. Eastman, and M. Aono, Solid State Commun. **31**, 917 (1979).

[11] P. K. Larsen, J. H. Neave, and B. A. Joyce, J. Phys. C **14**, 167 (1981).

[12] T. Hayashi, M. Tanaka, T. Nishinaga, H. Shimada, H. Tsuchiya, and Y. Otuka, J. Cryst. Growth **175/176**, 1063 (1997).

[13] H. Ohno, A. Shen, F. Matsukura, A. Oiwa, A. Endo, S. Katsumoto, and Y. Iye, Appl. Phys. Lett. **69**, 363 (1996).

[14] W. Gudat and D. E. Eastman, J. Vac. Sci. Technol. **13**, 831 (1976).

[15] F. Ciccacci and G. Chiaia, J. Vac. Sci. Technol. A **9**, 2991 (1991).

[16] T. C. Chiang, R. Ludeke, M. Aono, G. Landgren, F. J. Himpsel, and D. E. Eastman, Phys. Rev. B **27**, 4770 (1983).

[17] J.-J. Yeh and I. Lindau, At. Data Nucl. Data Tables **32**, 1 (1985).

[18] M. Linnarsson, E. Janzen, B. Monemar, M. Kleverman, and A. Thilderkvist, Phys. Rev. B **55**, 6938 (1997).

[19] K. C. Pandey and J. C. Phillips, Phys. Rev. B **9**, 1552 (1974).

[20] T. Mizokawa (unpublished).

[21] F. C. Zhang and T. M. Rice, Phys. Rev. B **37**, 3759 (1988); L. H. Tjeng *et al.*, Phys. Rev. Lett. **78**, 1126 (1997).

[22] T. Dietl, Science **287**, 1019 (2000).

[23] C. Benoit a la Guillaume, D. Scalbert, and T. Dietl, Phys. Rev. B **46**, 9853 (1992).

[24] J. H. Park, S. K. Kwon, and B. I. Min, Physica B **281-282**, 703 (2000).